Open access • Posted Content • DOI:10.1101/2021.06.11.448114

Mechanisms for Electron Uptake by Methanosarcina acetivorans During Direct Interspecies Electron Transfer — Source link

Dawn E. Holmes, Dawn E. Holmes, Jinjie Zhou, Jinjie Zhou ...+3 more authors

Institutions: Western New England University, University of Massachusetts Amherst, Shenzhen University

Published on: 11 Jun 2021 - bioRxiv (Cold Spring Harbor Laboratory)

Topics: Methanosarcina acetivorans, Methanosarcina, Methanogen, Syntrophy and Archaea

Related papers:

- Mechanisms for Electron Uptake by Methanosarcina acetivorans during Direct Interspecies Electron Transfer.
- Correlation of Key Physiological Properties of Methanosarcina Isolates with Environment of Origin.
- Methanobacterium Capable of Direct Interspecies Electron Transfer.
- Energy Conservation and Hydrogenase Function in Methanogenic Archaea, in Particular the Genus Methanosarcina.
- Metatranscriptomic Evidence for Direct Interspecies Electron Transfer Between Geobacter and Methanothrix Species in Methanogenic Rice Paddy Soils

Share this paper:

View more about this paper here: https://typeset.io/papers/mechanisms-for-electron-uptake-by-methanosarcina-acetivorans-4nxl8emwuk

bioRxiv preprint doi: https://doi.org/10.1101/2021.06.11.448114; this version posted June 11, 2021. The copyright holder for this preprint (which was not certified by peer review) is the author/funder, who has granted bioRxiv a license to display the preprint in perpetuity. It is made available under aCC-BY-NC-ND 4.0 International license.

1 Mechanisms for Electron Uptake by *Methanosarcina acetivorans* During Direct
2 Interspecies Electron Transfer
3
4 Dawn E. Holmes[1,2†]*, Jinjie Zhou[1,3*], Toshiyuki Ueki[1], Trevor Woodard[1], and Derek R.
5 Lovley[1]
6
7 1. Department of Microbiology, University of Massachusetts-Amherst, Amherst, MA,
8 USA
9 2. Department of Physical and Biological Science, Western New England University,
10 Springfield, MA, USA
11 3. Institute for Advanced Study, Shenzhen University, Shenzhen, Guangdong, China
12
13
14 *Both authors contributed equally
15 [†]Corresponding author
16 Dawn Holmes dholmes@wne.edu
17 Keywords: anaerobic respiration, extracellular electron transfer, *Methanosarcina*,
18 *Geobacter*, direct interspecies electron transfer (DIET), Rnf complex, *c*-type
19 cytochrome, methanogen, archaea
20 Running title: Methanogen outer-surface cytochrome facilitates DIET
21
22
23
24
25
26
27

bioRxiv preprint doi: https://doi.org/10.1101/2021.06.11.448114; this version posted June 11, 2021. The copyright holder for this preprint (which was not certified by peer review) is the author/funder, who has granted bioRxiv a license to display the preprint in perpetuity. It is made available under aCC-BY-NC-ND 4.0 International license.

28 **Abstract**

29 Direct interspecies electron transfer (DIET) between bacteria and methanogenic archaea
30 appears to be an important syntrophy in both natural and engineered methanogenic
31 environments. However, the electrical connections on the outer surface of methanogens
32 and the subsequent processing of electrons for carbon dioxide reduction to methane are
33 poorly understood. Here we report that the genetically tractable methanogen
34 *Methanosarcina acetivorans* can grow via DIET in co-culture with *Geobacter*
35 *metallireducens* serving as the electron-donating partner. Comparison of gene expression
36 patterns in *M. acetivorans* grown in co-culture versus pure culture growth on acetate
37 revealed that transcripts for the outer-surface, multi-heme, *c*-type cytochrome MmcA
38 were higher during DIET-based growth. Deletion of *mmcA* inhibited DIET. The high
39 aromatic amino acid content of *M. acetivorans* archaellins suggests that they might
40 assemble into electrically conductive archaella. A mutant that could not express archaella
41 was deficient in DIET. However, this mutant grew in DIET-based co-culture as well as
42 the archaella-expressing parental strain in the presence of granular activated carbon,
43 which was previously shown to serve as a substitute for electrically conductive pili as a
44 conduit for long-range interspecies electron transfer in other DIET-based co-cultures.
45 Transcriptomic data suggesting that the membrane-bound Rnf, Fpo, and HdrED
46 complexes also play a role in DIET were incorporated into a charge-balanced model
47 illustrating how electrons entering the cell through MmcA can yield energy to support
48 growth from carbon dioxide reduction. The results are the first genetics-based functional
49 demonstration of likely outer-surface electrical contacts for DIET in a methanogen.

50

51 **Importance**

bioRxiv preprint doi: https://doi.org/10.1101/2021.06.11.448114; this version posted June 11, 2021. The copyright holder for this preprint (which was not certified by peer review) is the author/funder, who has granted bioRxiv a license to display the preprint in perpetuity. It is made available under aCC-BY-NC-ND 4.0 International license.

52 The conversion of organic matter to methane plays an important role in the global carbon
53 cycle and is an effective strategy for converting wastes to a useful biofuel. The reduction
54 of carbon dioxide to methane accounts for approximately a third of the methane produced
55 in anaerobic soils and sediments as well as waste digesters. Potential electron donors for
56 carbon dioxide reduction are H_2 or electrons derived from direct interspecies electron
57 transfer (DIET) between bacteria and methanogens. Elucidating the relative importance
58 of these electron donors has been difficult due to a lack of information on the electrical
59 connects on the outer surface of methanogens and how they process the electrons
60 received from DIET. Transcriptomic patterns and gene deletion phenotypes reported here
61 provide insight into how a group of *Methanosarcina* that play an important role in
62 methane production in soils and sediments participate in DIET.

63

64

65 **Introduction**

66 The pathways for carbon and electron flux in methanogenic environments are of interest
67 because of the biogeochemical significance of methane production in diverse soils and
68 sediments as well as the importance of anaerobic digestion as a bioenergy strategy (1, 2).
69 Diverse communities of bacteria convert complex organic matter primarily to acetate and
70 carbon dioxide that are then converted by methanogenic archaea to methane. Low-
71 potential electrons derived from the oxidation of organic compounds to acetate and
72 carbon dioxide are delivered from the bacterial community to methanogens to provide the
73 necessary reducing power for the reduction of carbon dioxide to methane.

74 Two fundamentally different mechanisms for this interspecies electron transfer
75 are known. In direct interspecies electron transfer (DIET), electron-donating microbes

bioRxiv preprint doi: https://doi.org/10.1101/2021.06.11.448114; this version posted June 11, 2021. The copyright holder for this preprint (which was not certified by peer review) is the author/funder, who has granted bioRxiv a license to display the preprint in perpetuity. It is made available under aCC-BY-NC-ND 4.0 International license.

76 and methanogens establish direct electrical connections that enable electron transfer from
77 the electron-donating partner to the methanogen to support carbon dioxide reduction (2-
78 4). In interspecies H_2 transfer, the electron-donating partner transfers electrons to protons,
79 generating H_2, which functions as a diffusive electron carrier to H_2-utilizing
80 methanogens, which oxidize the H_2 to harvest electrons for carbon dioxide reduction (5-
81 7). Formate can also serve as a substitute for H_2 (6, 8, 9).

82 The relative importance of DIET and interspecies H_2/formate transfer in
83 methanogenic soils/sediments or most anaerobic digesters is unknown. Measurements of
84 H_2 turnover rates in methanogenic soils, sediments, and anaerobic digesters accounted for
85 less than 10% of the electron flux required for the observed rates of carbon dioxide
86 reduction to methane (10-12), suggesting that H_2 exchange was not the primary route for
87 interspecies electron transfer (13). Those results do not rule out interspecies formate
88 exchange, but rapid exchange between formate and H_2/carbon dioxide in methanogenic
89 environments prevents accurate assessment of formate fluxes (14). The relatively low
90 reported rates of H_2 turnover are consistent with DIET, but a method for directly
91 measuring the electron fluxes between cells in complex environments has not yet been
92 developed.

93 An alternative strategy for elucidating the significance of interspecies H_2/formate
94 transfer and DIET might be to extrapolate from the composition of the microbial
95 community and transcriptional or proteomic data (15-17). For example, *in situ* gene
96 expression patterns of *Geobacter* and *Methanothrix* species, which were abundant in
97 methanogenic rice paddy soils, suggested that they were participating in DIET (17). The
98 likely participation of paddy-soil *Geobacter* species in DIET could be surmised from

bioRxiv preprint doi: https://doi.org/10.1101/2021.06.11.448114; this version posted June 11, 2021. The copyright holder for this preprint (which was not certified by peer review) is the author/funder, who has granted bioRxiv a license to display the preprint in perpetuity. It is made available under aCC-BY-NC-ND 4.0 International license.

99 high levels of expression for electrically conductive pili (e-pili) and a *c*-type cytochrome
100 known to be important for DIET. High expression of genes for carbon dioxide reduction
101 in *Methanothrix* species, which are unable to use H_2 or formate as electron donors,
102 indicated that *Methanothrix* species were one of the electron-accepting partners for DIET.
103 However, such analyses are far from comprehensive, in part because the full diversity of
104 microbes that can participate in DIET is poorly understood. New genera of bacteria and
105 methanogens capable of DIET are increasingly being identified (18-20). Furthermore,
106 gene expression patterns diagnostic for ongoing DIET need to be elucidated for
107 microorganisms, such as *Syntrophus* (18) and some *Methanosarcina* species (16, 19, 21-
108 23) that have the physiological flexibility to participate in either DIET or interspecies
109 H_2/formate transfer.

110 Comparative transcriptomic analysis of *M. barkeri* growing via DIET versus
111 interspecies H_2 transfer, revealed potential routes for intracellular electron flux for DIET
112 that employ protein complexes and electron carriers that are also important for the
113 conversion of carbon dioxide to methane with H_2 as the electron donor (21). Outer-
114 surface electrical contacts for DIET were not definitively identified. *M. barkeri* lacks
115 multi-heme outer-surface *c*-type cytochromes (24) that are important electrical contacts
116 for extracellular electron exchange in some bacteria and archaea (13). *M. mazei*, which
117 like *M. barkeri*, can reduce carbon dioxide with electrons derived from H_2 or DIET, has a
118 gene for a five-heme, *c*-type cytochrome, but deletion of the cytochrome gene did not
119 negatively impact DIET (19).

120 *M. barkeri* and *M. mazei* are physiologically classified as Type I *Methanosarcina*
121 (22). Key physiological characteristics of Type I *Methanosarcina* are the ability to use H_2

bioRxiv preprint doi: https://doi.org/10.1101/2021.06.11.448114; this version posted June 11, 2021. The copyright holder for this preprint (which was not certified by peer review) is the author/funder, who has granted bioRxiv a license to display the preprint in perpetuity. It is made available under aCC-BY-NC-ND 4.0 International license.

122 as an electron donor for carbon dioxide reduction as well as for energy conservation from
123 the conversion of acetate to methane via intracellular H_2 cycling. Although Type I
124 *Methanosarcina* can serve as the electron-accepting partner for DIET, they are typically
125 most abundant in high energy environments with relatively fast rates of organic carbon
126 turnover in which H_2 is more likely to be an intermediate in interspecies electron transfer
127 (22).

128 In contrast, Type II *Methanosarcina* predominate in more stable, steady-state
129 environments with slower rates of organic matter metabolism likely to favor DIET (22).
130 Key physiological characteristics of Type II *Methanosarcina* include the inability to use
131 H_2 as an electron donor, energy conservation during acetate metabolism via an Rnf
132 complex, and the presence of an outer-surface multi-heme *c*-type cytochrome that is
133 important for electron transfer to extracellular electron acceptors (22). The inability of
134 Type II *Methanosarcina* to utilize H_2 or formate as an electron donor for carbon dioxide
135 reduction, but to participate in DIET (22) is expected to simplify the study of their routes
136 for electron flux during DIET.

137 In order to better understand DIET mechanisms in Type II *Methanosarcina*, we
138 investigated DIET in *M. acetivorans*. *M. acetivorans* is the most well-studied Type II
139 *Methanosarcina* and is genetically tractable (25-28). Transcriptomic and gene deletion
140 studies (29) demonstrated that its multi-heme outer-surface *c*-type cytochrome MmcA is
141 important for extracellular electron transfer to the humic substances analogue
142 anthraquinone-2,6-disulfonate (AQDS). Here we report that *M. acetivorans* can function
143 as the electron-accepting partner for DIET and provide insights into mechanisms for
144 electron uptake and energy conservation during DIET-based growth.

bioRxiv preprint doi: https://doi.org/10.1101/2021.06.11.448114; this version posted June 11, 2021. The copyright holder for this preprint (which was not certified by peer review) is the author/funder, who has granted bioRxiv a license to display the preprint in perpetuity. It is made available under aCC-BY-NC-ND 4.0 International license.

145 **Results and Discussion**

146 ***Methanosarcina acetivorans* can participate in DIET**

147 Co-cultures of *M. acetivorans* and *G. metallireducens* metabolized ethanol to
148 methane. As previously observed with co-cultures of *G. metallireducens* and other
149 electron-accepting partners (16, 30, 31), an adaption period of 38-45 days was required
150 for substantial methane to be produced in the initial co-culture. However, with
151 subsequent transfer, ethanol was converted to methane without a substantial lag (Figure
152 1).

153 After four transfers of the co-culture, the methane yield was 1.1 mol CH_4/mol
154 ethanol. Stoichiometric conversion of ethanol to methane yields 1.5 moles of methane,
155 but a portion of the carbon and electrons is required for biomass production. The methane
156 yield in the *G. metallireducens/M. acetivorans* co-culture falls within the range of 0.91
157 mol CH_4/mol ethanol to 1.31 mol CH_4/mol ethanol yields which were obtained when *G.*
158 *metallireducens* was the electron donating partner for co-cultures grown with other
159 acetotrophic methanogens, such as *Methanothrix harundinacea*, *M. barkeri*, *M. mazei, M.*
160 *vacuolata, M. horonobensis*, and *M. subterranea* (16, 19, 22, 23, 31).

161 Genes for enzymes specific to the carbon dioxide reduction pathway were more
162 highly expressed in *M. acetivorans* growing in co-culture with *G. metallireducens* versus
163 cells growing in pure culture on acetate (Figure 2, Supplementary Table S1a). This result
164 is in accordance with the fact that carbon dioxide reduction is required to consume the
165 electrons released from ethanol metabolism, accounting for one-third of the methane
166 produced during DIET. Little or no carbon dioxide reduction is expected during growth
167 solely on acetate. H_2 or formate cannot be the interspecies electron carrier between *G.*

bioRxiv preprint doi: https://doi.org/10.1101/2021.06.11.448114; this version posted June 11, 2021. The copyright holder for this preprint (which was not certified by peer review) is the author/funder, who has granted bioRxiv a license to display the preprint in perpetuity. It is made available under aCC-BY-NC-ND 4.0 International license.

168 *metallireducens* and *M. acetivorans* for carbon dioxide reduction because *G.*
169 *metallireducens* cannot grow by metabolizing ethanol with the formation of H_2 or
170 formate (32) and *M. acetivorans* is unable to use H_2 or formate as an electron donor (33).
171 Quantitative PCR of DNA extracted from the 4th transfer of triplicate co-cultures
172 with primers targeting the 16S rRNA genes of *G. metallireducens* and *M. acetivorans*
173 revealed that *G. metallireducens* accounted for 60 $\pm$ 10% (mean $\pm$ standard deviation) of
174 the cells in the co-culture. Confocal and transmission electron microscopy also indicated
175 a near-equal abundance of the two species (Figure 3a,b), and revealed that both species
176 were typically in close proximity, often with more than one cell of each species adjacent
177 to its DIET partner (Figure 3a,b).

178 **Potential Role(s) for the Archaellum in DIET**

179 Higher magnification TEM images provided further insights into the interactions
180 between *G. metallireducens* and *M. acetivorans* (Figure 3c-e). The outer surfaces of cells
181 of the two species often appeared to be in direct contact (Figure 3c,d). However, there
182 were instances in which filaments (diameter ca. 15 nm), consistent with the appearance of
183 the *M. acetivorans* archaellum (33), appeared to emanate from *M. acetivorans* and
184 connect to juxtaposed cells of *G. metallireducens* (Figure 3e,f).
185 Genes coding for archaella proteins were not more significantly expressed in
186 DIET- versus acetate-grown cells (Supplementary Table S1) as might be expected
187 because *M. acetivorans* also expresses archaella during growth on acetate (33). In order
188 to evaluate whether the *M. acetivorans* archaella might play a role in DIET, a strain in
189 which two genes for puative archaellin proteins, FlaB1 and FlaB2, were deleted, yielding
190 a strain that did not express archaella (Supplementary Figure S1d). The archaella-

bioRxiv preprint doi: https://doi.org/10.1101/2021.06.11.448114; this version posted June 11, 2021. The copyright holder for this preprint (which was not certified by peer review) is the author/funder, who has granted bioRxiv a license to display the preprint in perpetuity. It is made available under aCC-BY-NC-ND 4.0 International license.

191 deficient strain did not form an effective DIET co-culture with *G. metallireducens* for
192 over 150 days (Figure 4a). However, when the co-cultures were amended with granular
193 activated carbon (GAC), the co-cultures initated with the archaella-deficeint strain
194 produced methane as effectively as co-cultures initated with the parent *M. acetivorans*
195 strain that expressed archaella (Figure 4b).

196 GAC and other electrically conductive carbon materials can stimulate DIET
197 between wild-type partners and can enable DIET when genes for key extracellular
198 electron transport proteins that are otherwise essential for DIET, like e-pili, have been
199 deleted (34-37). The DIET partners attach to the GAC rather than each other and the
200 GAC serves as the conduit for long-range interspecies electron transfer (13). Archaella
201 are homologous to type IV pili (38) and the archaellum of *Methanospirillum hungatei* has
202 a conductance 4-fold higher than *G. sulfurreducens* e-pili, demonstrating that at least
203 some archaella can be electrically conductive and might have the potential to be involved
204 in cell-to-cell electron transfer (39). The conductivity of a diversity of e-pili as well as the
205 *Ms. hungatei* archaellum are associated with a high abundance of aromatic amino acids
206 (> 9 %) in the pilin/archaellin monomers and no large gaps (> 40 amino acids) without
207 aromatic amino acids (18). The high density of aromatic amino acids (FlaB1, 11.3%;
208 FlaB2, 9.5%) and the lack of large aromatic-free gaps (largest gaps: FlaB1, 26 amino
209 acids; FlaB2, 29 amino acids) in the *M. acetivorans* archaellins suggest that they might
210 yield conductive archaella. The ability of GAC to rescue the archaella-deficient strain to
211 enable DIET is consistent with a possible archaella role in long-range electron transport.
212 However, other, more traditional roles of archaella, such as conferring motility and
213 facilitating attachment (40) might also help cells locate a DIET partner and/or establish

bioRxiv preprint doi: https://doi.org/10.1101/2021.06.11.448114; this version posted June 11, 2021. The copyright holder for this preprint (which was not certified by peer review) is the author/funder, who has granted bioRxiv a license to display the preprint in perpetuity. It is made available under aCC-BY-NC-ND 4.0 International license.

214 initial interspecies contact. In order to more definitively evaluate a role for the *M.*
215 *acetivorans* archaellum in interspecies electron transfer it will be necessary to follow the
216 approach employed for evaluating the role of *Geobacter* e-pili in DIET (37) and construct
217 a strain that expresses an archaellum of with potentially low conductivity. However, such
218 studies are technically difficult and well beyond the scope of the current investigation.
219

220 **A Role for the Outer-Surface Cytochrome MmcA**

221 Gene expression and deletion studies have indicated that the outer surface multi-
222 heme *c*-type cytochrome MmcA is an important component in *M. acetivorans* for
223 electron transfer to the extracellular electron acceptor AQDS (29). Gene transcripts for
224 MmcA were 5-fold higher (p=0.008) during growth via DIET versus growth on acetate
225 (Figure 2, Supplementary Table S1). Methane production was inhibited in co-cultures
226 initiated with an MmcA-deficient strain of *M. acetivorans* for over 150 days (Figure 4a).
227 These results suggest that MmcA may provide an important route for extracellular
228 electron exchange during DIET.

229 Unlike the archaella-deficient mutant, GAC did not rapidly rescue the growth of
230 the MmcA-deficient mutant in co-culture (Figure 4b). The co-cultures initiated with the
231 MmcA-deficient strain only grew after a very long lag period. The poor methane
232 production even in the presence of GAC is consistent with the fact that MmcA is thought
233 to be embedded in the membrane of *M. acetivorans* (25, 41). Thus, its role in
234 extracellular electron transfer is expected to be facilitating transmembrane electron
235 transport. Although GAC can enhance long-range electron exchange between the outer

bioRxiv preprint doi: https://doi.org/10.1101/2021.06.11.448114; this version posted June 11, 2021. The copyright holder for this preprint (which was not certified by peer review) is the author/funder, who has granted bioRxiv a license to display the preprint in perpetuity. It is made available under aCC-BY-NC-ND 4.0 International license.

236 cell surface of different species, it does not have a conceivable role in electron transfer
237 across the cell membrane.
238 *M. acetivorans* has genes for four other putative *c*-type cytochromes, but the
239 presence of these proteins in *M. acetivorans* has yet to be verified and deletion of the
240 genes for each of the four cytochrome genes had no impact on extracellular electron
241 transfer to AQDS even though several of the genes had higher transcript abundance when
242 grown with AQDS as the electron acceptor (29). Transcript abundance for three of these
243 putative cytochrome genes (MA0167, MA2925, MA3739) was higher in DIET-grown *M.*
244 *acetivorans* than in acetate-grown cells (Supplementary Table S1). Further studies to
245 attempt to document the expression of these proteins in *M. acetivorans* are warranted.
246

247 **Potential role for Rnf and Fpo Complexes in DIET**

248 MmcA has the potential to exchange electrons with methanophenazine or the
249 membrane-bound Rnf complex RnfCDGEAB (25, 42-44). Methanophenazine is an
250 important membrane-bound electron carrier and the Rnf complex is physically associated
251 with MmcA in the *M. acetivorans* membrane (25, 41). The Rnf complex oxidizes reduced
252 ferrodoxin with concomitant transport of sodium across the cell membrane from the cell
253 interior to exterior (25, 42). It is proposed that the electrons from ferrodoxin oxidation are
254 transferred directly to methanophenazine during acetotrophic methanogenesis (25, 42,
255 45) or to MmcA during reduction of extracellular electron acceptors such as Fe(III) and
256 AQDS (25, 29, 46).
257 Transcripts for the majority of genes coding for Rnf subunits were more
258 significantly expressed in DIET-grown cells than acetate-grown cells (Figure 2,

bioRxiv preprint doi: https://doi.org/10.1101/2021.06.11.448114; this version posted June 11, 2021. The copyright holder for this preprint (which was not certified by peer review) is the author/funder, who has granted bioRxiv a license to display the preprint in perpetuity. It is made available under aCC-BY-NC-ND 4.0 International license.

259 Supplementary Table S2), suggesting an enhanced role for the Rnf complex during DIET.
260 It seems possible that during DIET the Rnf complex functions in the reverse direction
261 proposed for extracellular electron transfer, i.e. accepting electrons to generate the
262 reduced ferrodoxin that is required for the first step in the reduction of carbon dioxide to
263 methane (Figure 2). The most likely electron donor to the Rnf complex is MmcA, which
264 is thought to exchange electrons with Rnf in other forms of *M. acetivorans* electron
265 transfer (25) and, as noted above, is important for DIET (Figure 2). The ferrodoxin
266 reduction requires transfer of sodium to the interior of the cell via the Rnf complex
267 (Figure 2). Ten genes coding for ferredoxin proteins and a gene coding for an unusual
268 flavodoxin (FldA) that can replace ferredoxin as an electron donor under iron-limiting
269 conditions (47) were more than 2 fold more highly expressed ($p<0.05$) in DIET-grown
270 cells (Supplementary Table S1).

271 Although the pathway for the biosynthesis of methanophenazine has not been
272 deciphered yet, it resembles respiratory quinones in that it has a polyprenyl side-chain
273 connected to a redox-active moiety (48, 49). Geranylfarnesyl diphosphate is a
274 biosynthetic precursor of methanophenazine, and a homolog (MA0606) of the
275 geranylfarnesyl diphosphate synthase (MM0789) required for methanophenazine
276 biosynthesis in *M. mazei* (50) was 2.42-fold ($p=0.01$) more highly expressed in DIET
277 grown cells (Supplementary Table S1).

278 The pathway for carbon dioxide reduction to methane also requires reduced F_{420}
279 (51). The membrane-bound F_{420} dehydrogenase of *M. barkeri* can accept electrons from
280 reduced methanophenazine to generate reduced F_{420} (52) and has been proposed to
281 catalyze F_{420} reduction in a similar manner during *M. barkeri* DIET-based growth (21).

bioRxiv preprint doi: https://doi.org/10.1101/2021.06.11.448114; this version posted June 11, 2021. The copyright holder for this preprint (which was not certified by peer review) is the author/funder, who has granted bioRxiv a license to display the preprint in perpetuity. It is made available under aCC-BY-NC-ND 4.0 International license.

282 This reaction requires concomitant proton translocation from the outside of the cell to the
283 cell interior. Genes for all but one of the Fpo subunits were more highly expressed during
284 *M. acetivorans* growth via DIET versus growth on acetate (Figure 2; Supplementary
285 Table S3). Therefore, electron transfer from MmcA to methanophenazine followed by
286 electron transfer to Fpo is a likely route for generating $F_{420}H_2$ to support carbon dioxide
287 reduction during DIET (Figure 2).

288 As in other methanogens, methane production in *M. acetivorans* also requires an
289 electron donor to reduce Coenzyme M 7-mercaptoheptanoylthreonine-phosphate
290 heterodisulfide (CoMS-SCoB) to regenerate coenzyme M (25). It is proposed that during
291 acetoclastic growth the membrane-bound HdrED complex accepts electrons from
292 methanophenazine reduced by the Rnf complex to reduce CoMS-SCoB to HSCoM and
293 HSCoB while pumping two protons from the interior of the cell across the cell membrane
294 (25). Even though the HdrED complex is required for the conversion of acetate to
295 methane, genes for components of this complex were more highly expressed during
296 growth via DIET (Figure 2, Supplementary Table S4). Thus, HdrED is a likely catalyst
297 for CoMS-SCoB reduction (Figure 2). An alternative strategy for reducing CoMS-SCoB
298 is for HdrABC complexes to oxidize $F_{420}H_2$ in an electron bifurcation reaction that
299 reduces both ferrodoxin and CoMS-SCoB (53, 54). Genes for components of the *M.*
300 *acetivorans* HdrABC complexes were more highly expressed in DIET-grown cells,
301 suggesting the possibility for multiple routes for electron flux during DIET
302 (Supplementary Table S4).

303 The proposed route for electron flux during DIET (Figure 2) demonstrates the
304 possibility for energy conservation from carbon dioxide reduction to methane with

bioRxiv preprint doi: https://doi.org/10.1101/2021.06.11.448114; this version posted June 11, 2021. The copyright holder for this preprint (which was not certified by peer review) is the author/funder, who has granted bioRxiv a license to display the preprint in perpetuity. It is made available under aCC-BY-NC-ND 4.0 International license.

305 electrons derived from DIET. The oxidation of two ethanols to acetate and carbon
306 dioxide yields eight electrons required to reduce carbon dioxide to methane. The eight
307 protons that are also generated from this ethanol metabolism must be consumed in order
308 to prevent acidification within the DIET aggregates. Half of these protons are consumed
309 with the proposed Fpo generation of $F_{420}H_2$ (Figure 2). External sodium ions are needed
310 for the proposed Rnf generation of reduced ferrodoxin. This requirement can be met by
311 the H^+/Na^+ antiporter complex (MrpABCDEFG), which adjusts the H^+/Na^+ ratio for
312 optimal ATP synthesis by A_1A_0 ATP synthase (55, 56). As might be expected, genes for
313 components of this complex are more highly expressed in DIET-grown cells (Figure 2,
314 Supplementary Table S2). The proposed consumption of ten positive charges in the
315 reactions catalyzed by the Fpo and Rnf complexes consumes two more positive charges
316 than the eight that are available from ethanol metabolism. However, the export of two
317 sodiums during the reaction catalyzed by the MtrA-H complex and the two protons
318 exported by HdrED yields a net exterior proton gradient to support ATP generation via
319 ATPase. Detailed functional studies would be required to completely validate this model,
320 but the model is based on previously proposed functions of these *M. acetivorans*
321 components, supporting its feasibility.

322 **Implications**

323 The results demonstrate that *M. acetivorans* can serve as an electron-accepting
324 partner for DIET and reveal potential outer-surface electrical contacts and routes for
325 electron flux to support DIET-driven carbon dioxide reduction. This is significant
326 because *M. acetivorans*, which is genetically tractable and one of the most intensively
327 studied methanogens (25), is an excellent physiological model for the Type II

bioRxiv preprint doi: https://doi.org/10.1101/2021.06.11.448114; this version posted June 11, 2021. The copyright holder for this preprint (which was not certified by peer review) is the author/funder, who has granted bioRxiv a license to display the preprint in perpetuity. It is made available under aCC-BY-NC-ND 4.0 International license.

328 *Methanosarcina* species that are abundant in many methanogenic soils, sediments, and
329 subsurface environments (22). The results also suggest that different genera of
330 methanogens are likely to employ different strategies for electron uptake during growth
331 via DIET. For example, although MmcA appears to be important for *M. acetivorans*
332 DIET, some *Methanothrix* (31) and *Methanobacterium* (20) species can participate in
333 DIET, but lack *c*-type cytochromes (24).

334 DIET mechanisms in *M. acetivorans* also appear to differ significantly from those
335 described in *M. barkeri* (21). This is consistent with other substantial differences
336 between Type I (i.e. *M. barkeri*) and Type II (i.e. *M. acetivorans*) *Methanosarcina*
337 species (22). *M. barkeri* lacks MmcA and other *c*-type cytochromes (24). The lack of an
338 Rnf complex in *M. barkeri* requires that electron transport through the membrane to
339 generate reducing equivalents for carbon dioxide reduction relies on the Fpo complex
340 (21).

341 The diversity of mechanisms for DIET in methanogens suggests that the strategies that
342 rely on gene expression patterns to evaluate the importance of DIET in methanogenic
343 systems will need to accommodate these differences. The mechanisms for extracellular
344 electron exchange in the bacteria and archaea that predominate in anaerobic
345 environments such as soils, sediments, anaerobic digesters, and intestinal systems are still
346 poorly understood (13). For example, although multiple lines of evidence suggest that e-
347 pili are important for extracellular electron transfer in some *Geobacter* species, a model
348 for how e-pili interact with the rest of the *Geobacter* electron transport chain, which
349 could aid in understanding how the archaellum of *M. acetivorans* might ‘plug in’ to
350 membrane electron transport components during DIET, is not yet available (13).

bioRxiv preprint doi: https://doi.org/10.1101/2021.06.11.448114; this version posted June 11, 2021. The copyright holder for this preprint (which was not certified by peer review) is the author/funder, who has granted bioRxiv a license to display the preprint in perpetuity. It is made available under aCC-BY-NC-ND 4.0 International license.

351 However, the genetic tractability of *M. acetivorans* and the growing information on the
352 biochemistry and function of its key proteins (25); as well as its ability to grow as either
353 an electrogen (transporting electrons to extracellular electron acceptors) (29, 46), or an
354 electrotroph (consuming electrons from an external source), as shown here, suggest that
355 *M. acetivorans* is an excellent model microbe for further study of extracellular electron
356 exchange in archaea.

357 **Materials and Methods**

358 **Parental strain adaption for co-culture at a compatible salinity**

359 *Geobacter metallireducens* (ATCC 53774) was routinely cultured at 30°C under
360 anaerobic conditions (N_2:CO_2, 80:20, vol/vol) with ethanol (20 mM) provided as the
361 electron donor and Fe(III) citrate (56 mM) as the electron acceptor in freshwater medium
362 as previously described (57). *M. acetivorans* strain WWM1 (Δ*hpt*) (58), (a gift from
363 William Metcalf at the University of Illinois) was routinely cultured at 37°C in HS-
364 methanol-acetate medium under strict anaerobic conditions as previously described (27,
365 59).

366 In order to obtain strains of both microbes that grew at compatible temperatures
367 and salinities, both cultures were adapted to grow at 30°C in MA medium which
368 consisted of the following components per liter: 0.35 g K_2HPO_4, 0.23 g KH_2PO_4, 0.5 g
369 NH_4Cl, 4 g NaCl, 1 ml 0.2% wt/vol $FeSO_4$, 1 ml trace element solution SL-10 (DSMZ
370 culture collection, medium 320), 10 mM $NaHCO_3$, 10 ml Wolin's vitamin solution
371 (DSMZ culture collection, medium 141), 0.3 mM L-cysteine·HCl, 1 ml 2.7% $CaCl_2 \cdot 2$
372 H_2O, and 1 ml 4.5% $MgSO_4 \cdot 7$ H_2O. The sodium bicarbonate, Wolin's vitamins, L-

bioRxiv preprint doi: https://doi.org/10.1101/2021.06.11.448114; this version posted June 11, 2021. The copyright holder for this preprint (which was not certified by peer review) is the author/funder, who has granted bioRxiv a license to display the preprint in perpetuity. It is made available under aCC-BY-NC-ND 4.0 International license.

373 cysteine, $CaCl_2$, and $MgSO_4$ solutions were added from sterile anoxic stocks after the
374 base medium was autoclaved.
375 For co-culture experiments, *G. metallireducens* and *M. acetivorans* were grown
376 with 20 mM ethanol provided as the electron donor and carbon dioxide as the electron
377 acceptor at 30°C in MA media as previously described (16, 21). For comparative
378 transcriptomic studies *M. acetivorans* was also grown in MA medium with acetate (40
379 mM) as the sole electron donor.

380 ***M. acetivorans* mutants**

381 A mutant strain in which the gene for the multi-heme *c*-type cytochrome MmcA was
382 deleted was described previously (29). A strain in which the genes for the archaellin
383 monomer proteins FlaB1 and FlaB2 were deleted was constructed by replacing *flaB1* and
384 *flaB2* genes with *pac* (puromycin resistance gene) (Supplementary Figure S1). The
385 upstream and downstream regions of *flaB1/flaB2* were amplified by PCR with the
386 following primer pairs:
387 TCTCTCGAGTTCCTTGAAGATATTAAAGGTC/TCTAAGCTTAATGAATCACCTC
388 AATATTGTG and
389 TCTGGATCCAGCTTGAAATCAAACCAC/TCTGCGGCCGCCACTGCAGCTATAA
390 CAC, respectively. The DNA fragments of the upstream and downstream regions were
391 digested with *XhoI/HindIII* and *BamHI/NotI*, respectively. The upstream fragment was
392 ligated with pJK3 (27) and then the downstream fragment was ligated with the pJK3
393 containing the upstream fragment. The constructed plasmid was linearized with *XhoI* and
394 the linearized plasmid was used for transformation. The deletion of *flaB1*/*flaB2* was
395 verified by PCR with primer pairs, TCTCTCGAGTTCCTTGAAGATATTAAAGGTC

bioRxiv preprint doi: https://doi.org/10.1101/2021.06.11.448114; this version posted June 11, 2021. The copyright holder for this preprint (which was not certified by peer review) is the author/funder, who has granted bioRxiv a license to display the preprint in perpetuity. It is made available under aCC-BY-NC-ND 4.0 International license.

396 (P1)/CCGCCTGCAGTATTCGTTAC (P3) and ACTCTATGCTTGCAGCTGAC
397 (P4)/TCTGCGGCCGCCACTGCAGCTATAACAC (P2) (Supplementary Figure S1).
398 The replacement with the *pac* gene was verified by PCR with a primer pair,
399 AGAGACCCTATCTTACCTGC (P5)/ TCTGCGGCCGCCACTGCAGCTATAACAC
400 (P2) (Supplementary Figure S1). Absence of flagella in the deletion mutant strain was
401 confirmed with transmission electron microscopy (Supplementary Figure S1).

402 **Analytical techniques**

403 Ethanol in solution was monitored with a gas chromatograph equipped with a headspace
404 sampler and a flame ionization detector (Clarus 600; PerkinElmer Inc., CA). Methane in
405 the headspace was measured by gas chromatography with a flame ionization detector
406 (Shimadzu, GC-8A) as previously described (60). Acetate concentrations were measured
407 with a SHIMADZU high performance liquid chromatograph (HPLC) with an Aminex
408 HPX-87H Ion Exclusion column (300 mm × 7.8 mm) and an eluent of 8.0 mM sulfuric
409 acid.

410 **Microscopy**

411 Cells were routinely examined by phase-contrast and fluorescence microscopy (BV-2A
412 filter set) with a Nikon E600 microscope. For transmission electron microscopy (TEM), 7
413 µl of cells were dropcast on plasma-sterilized carbon coated 400 mesh copper ultralight
414 grids for 10 minutes. Liquid was wicked off and the grid was stained with 3 µL 2%
415 uranyl acetate for 15-20 seconds before the liquid was wicked off and air-dried.
416 Transmission electron microscopy was done on a FEI Tecnai 12 at 120kV, spot size 3,
417 with a camera exposure of 200 ms.

bioRxiv preprint doi: https://doi.org/10.1101/2021.06.11.448114; this version posted June 11, 2021. The copyright holder for this preprint (which was not certified by peer review) is the author/funder, who has granted bioRxiv a license to display the preprint in perpetuity. It is made available under aCC-BY-NC-ND 4.0 International license.

418 Cells for confocal microscopy were harvested (1mL) and vacuumed gently onto a
419 polycarbonate 0.2μm filter, washed with 1mL of wash buffer for 10 minutes, vacuumed,
420 stained with the Live/Dead BacLight Bacterial Viability kit (Thermofisher) (1mL
421 staining, 3 μL each stain per mL) for 10 minutes, vacuumed, destained with wash buffer
422 for 10 minutes, vacuumed, and mounted on glass slides with cover slips and antifade
423 reagent in glycerol. Cells were visualized on a Nikon A1R-SIMe confocal microscope.
424

425 **DNA extraction and quantitative PCR**

426 Genomic DNA was extracted from co-cultures with the MasterPure complete DNA
427 purification kit (Lucigen). The proportion of *G. metallireducens* and *M. acetivorans* cells
428 in co-cultures was determined with quantitative PCR using the following primer sets: (i)
429 GS15-16Sq-f (5'-CAGCTCGTGTCGTGAGATGT-3') and GS15-16Sq-r (5'-
430 GTTTGACACCGGCAGTTTCT-3') which amplified a 106 bp fragment from the 16S
431 rRNA gene of *G. metallireducens* and (ii) MA-16Sq-f (5'-
432 GTAGTCCCAGCCGTAAACGA-3') and MA-16Sq-r (5'-
433 CCCGCCAATTCCTTTAAGTT-3') which amplified a 132 bp fragment of the *M.*
434 *acetivorans* 16S rRNA gene. Both *G. metallireducens* and *M. acetivorans* have three
435 copies of the 16S rRNA gene in their genomes. Therefore, qPCR results were not
436 influenced by unequal gene copy numbers. Standard curve analysis of both primer sets
437 revealed that they had >95% efficiencies and melt curve analysis yielded a single peak
438 indicating that they were highly specific.
439 Power SYBR Green PCR Master Mix (Applied Biosystems, Foster City, CA) and
440 an ABI 7500 real-time PCR system were used to amplify and to quantify all PCR

bioRxiv preprint doi: https://doi.org/10.1101/2021.06.11.448114; this version posted June 11, 2021. The copyright holder for this preprint (which was not certified by peer review) is the author/funder, who has granted bioRxiv a license to display the preprint in perpetuity. It is made available under aCC-BY-NC-ND 4.0 International license.

441 products. Each reaction mixture (25 µl) consisted of forward and reverse primers at a
442 final concentration of 200 nM, 5 ng of gDNA, and 12.5 µl of Power SYBR Green PCR
443 Master Mix (Applied Biosystems).

444 **RNA Extraction**

445 Cells were harvested from triplicate 50 ml cultures of *M. acetivorans* grown alone with
446 acetate (40 mM) provided as a substrate (acetate conditions), or 50 ml cultures of *M.*
447 *acetivorans* grown in co-culture with *G. metallireducens* with ethanol (20 mM) provided
448 as an electron donor (DIET condition). Cells were harvested during mid-exponential
449 phase when ~18 mM methane was detected in the headspace.

450 Cells were split into 50 ml conical tubes (BD Sciences), mixed with RNA Protect
451 (Qiagen) in a 1:1 ratio, and pelleted by centrifugation at 3,000 x g for 15 minutes at 4ºC.
452 Pellets were then immediately frozen in liquid nitrogen and stored at -80 ºC. Total RNA
453 was extracted from cell pellets as previously described (61), and all six RNA samples (3
454 acetate, 3 DIET) were cleaned with the RNeasy Mini Kit (Qiagen) and treated with Turbo
455 DNA-free DNase (Ambion). PCR with primers targeting the 16S rRNA gene was then
456 done on all samples to ensure that they were not contaminated with genomic DNA.
457 mRNA was then further enriched from all samples with the MICROB*Express* kit
458 (Ambion), according to the manufacturer's instructions.

459 **Illumina sequencing and data analysis.**

460 The ScriptSeq™ v2 RNA-Seq Library Preparation Kit (Epicentre) was used to
461 prepare directional multiplex libraries. Paired end sequencing was then performed on
462 these libraries with a Hi-Seq 2000 platform at the Deep Sequencing Core Facility at the
463 University of Massachusetts Medical School in Worchester, Massachusetts.

bioRxiv preprint doi: https://doi.org/10.1101/2021.06.11.448114; this version posted June 11, 2021. The copyright holder for this preprint (which was not certified by peer review) is the author/funder, who has granted bioRxiv a license to display the preprint in perpetuity. It is made available under aCC-BY-NC-ND 4.0 International license.

464 Raw data was quality checked with FASTQC
465 (http://www.bioinformatics.babraham.ac.uk/projects/fastqc/), and initial raw non-filtered
466 forward and reverse sequencing libraries contained an average of 68,911,030 +/-
467 21,863,730 reads that were ~100 basepairs long (Supplementary Table S5). Sequences
468 from all of the libraries were trimmed and filtered with Trimmomatic (62) which yielded
469 an average of 55,239,290 +/- 29,060,121 quality reads per RNAseq library.
470 All paired-end reads were then merged with FLASH (63), resulting in 32,159,242
471 +/- 22,219,390 reads with an average read length of 134 +/- 28 basepairs. Ribosomal
472 RNA (rRNA) reads were then removed from the libraries with SortMeRNA (64), which
473 resulted in 4,959,312 +/- 2,340,361 mRNA reads.

474 **Mapping of mRNA reads**

475 Trimmed and filtered mRNA reads from the triplicate samples for the two
476 different culture conditions were mapped against the *M. acetivorans* strain C2A genome
477 (NC_003552) downloaded from IMG/MER (img.jgi.doe.gov) using ArrayStar software
478 (DNAStar). Reads were normalized and processed for differential expression studies
479 using the edgeR package in Bioconductor (65). All genes that were $\geq$2 fold differentially
480 expressed with p-values $\leq$ 0.05 are reported in Supplementary Table S1.

481 **Data Availability**

482 Illumina sequence reads have been submitted to the SRA NCBI database under
483 BioProject PRJNA727272 and Biosamples SAMN19011637, and SAMN19011638.

484 **Acknowledgments**

485 The confocal microscopy data was gathered in the Light Microscopy
486 Facility and Nikon Center of Excellence at the Institute for Applied

bioRxiv preprint doi: https://doi.org/10.1101/2021.06.11.448114; this version posted June 11, 2021. The copyright holder for this preprint (which was not certified by peer review) is the author/funder, who has granted bioRxiv a license to display the preprint in perpetuity. It is made available under aCC-BY-NC-ND 4.0 International license.

487 Life Sciences, UMass Amherst with support from the Massachusetts Life
488 Sciences Center. The transmission electron microscopy images were
489 collected in the Electron Microscopy Facility at the Institute for
490 Applied Life Sciences, UMass Amherst.

491 This research was supported by the Army Research Office and was accomplished
492 under Grant Number W911NF-17-1-0345. The views and conclusions contained in this
493 document are those of the authors and should not be interpreted as representing the
494 official policies, either expressed or implied, of the Army Research Office or the U.S.
495 Government.

496

497 **Ethics declarations**

498 The authors do not declare any conflicts of interest.

499

500 **References**

501 1. Whiticar M. 2020. The Biogeochemical Methane Cycle, p 669-746. *In* Wilkes H
502 (ed), Hydrocarbons, Oils and Lipids: Diversity, Origin, Chemistry and Fate,
503 Handbook of Hydrocarbons and Lipid Microbiology doi: DOI: 10.1007/978-3-
504 319-90569-3_5. Springer Nature, Switzerland.
505 2. Zhao Z, Li Y, Zhang Y, Lovley D. 2020. Sparking anaerobic digestion: promoting
506 direct interspecies electron transfer to enhance methane production. iScience
507 23:101794.
508 3. Lovley DR. 2017. Syntrophy goes electric: direct interspecies electron transfer.
509 Annu Rev Microbiol 71:643-664.
510 4. Rotaru AE, Yee MO, Musat F. 2021. Microbes trading electricity in consortia of
511 environmental and biotechnological significance. Curr Opin Biotechnol 67:119-
512 129.
513 5. Stams AJ, Plugge CM. 2009. Electron transfer in syntrophic communities of
514 anaerobic bacteria and archaea. Nat Rev Microbiol 7:568-77.
515 6. McInerney MJ, Struchtemeyer CG, Sieber J, Mouttaki H, Stams AJ, Schink B,
516 Rohlin L, Gunsalus RP. 2008. Physiology, ecology, phylogeny, and genomics of
517 microorganisms capable of syntrophic metabolism. Ann N Y Acad Sci 1125:58-
518 72.

bioRxiv preprint doi: https://doi.org/10.1101/2021.06.11.448114; this version posted June 11, 2021. The copyright holder for this preprint (which was not certified by peer review) is the author/funder, who has granted bioRxiv a license to display the preprint in perpetuity. It is made available under aCC-BY-NC-ND 4.0 International license.

519 7. Sieber JR, McInerney MJ, Gunsalus RP. 2012. Genomic insights into syntrophy:
520 the paradigm for anaerobic metabolic cooperation. Annu Rev Microbiol 66:429-
521 452.
522 8. Sieber JR, Le HM, McInerney MJ. 2014. The importance of hydrogen and
523 formate transfer for syntrophic fatty, aromatic and alicyclic metabolism. Environ
524 Microbiol 16:177-88.
525 9. Rotaru AE, Shrestha PM, Liu FH, Ueki T, Nevin K, Summers ZM, Lovley DR.
526 2012. Interspecies electron transfer via hydrogen and formate rather than direct
527 electrical connections in cocultures of *Pelobacter carbinolicus* and *Geobacter*
528 *sulfurreducens*. Appl Environ Microbiol 78:7645-7651.
529 10. Conrad R, Phelps TJ, Zeikus JG. 1985. Gas metabolism evidence in support of the
530 juxtaposition of hydrogen-producing and methanogenic bacteria in sewage sludge
531 and lake sediments. Appl Environ Microbiol 50:595-601.
532 11. Conrad R, Babbel M. 1989. Effect of dilution on methanogenesis, hydrogen
533 turnover and interspecies hydrogen transfer in anoxic paddy soil. FEMS
534 Microbiol Ecol 62:21-28.
535 12. Conrad R, Mayer HP, Wust M. 1989. Temporal change of gas metabolism by
536 hydrogen-syntrophic methanogenic bacterial associations in anoxic paddy soil.
537 FEMS Microbiol Ecol 62:265-273.
538 13. Lovley D, Holmes D. 2021. Electromicrobiology: The ecophysiology of
539 phylogenetically diverse electroactive microbes. Nat Rev Microbiol in press.
540 14. Lovley D, Klug M. 1982. Intermediary metabolism of organic carbon in the
541 sediment of a eutrophic lake. Appl Environ Microbiol 43:552-560.
542 15. Morita M, Malvankar NS, Franks AE, Summers ZM, Giloteaux L, Rotaru AE,
543 Rotaru C, Lovley DR. 2011. Potential for direct interspecies electron transfer in
544 methanogenic wastewater digester aggregates. MBio 2:e00159-11.
545 16. Rotaru AE, Shrestha PM, Liu F, Markovaite B, Chen S, Nevin KP, Lovley DR.
546 2014. Direct interspecies electron transfer between Geobacter metallireducens and
547 Methanosarcina barkeri. Appl Environ Microbiol 80:4599-605.
548 17. Holmes DE, Shrestha PM, Walker DJF, Dang Y, Nevin KP, Woodard TL, Lovley
549 DR. 2017. Metatranscriptomic evidence for direct interspecies electron transfer
550 between *Geobacter* and *Methanothrix* species in methanogenic rice paddy soils.
551 Appl Environ Microbiol 83:e00223-17.
552 18. Walker DJF, Nevin KP, Holmes DE, Rotaru AE, Ward JE, Woodard TL, Zhu J,
553 Ueki T, Nonnenmann SS, McInerney MJ, Lovley DR. 2020. Syntrophus
554 conductive pili demonstrate that common hydrogen-donating syntrophs can have
555 a direct electron transfer option. ISME J 14:837-846.
556 19. Yee MO, Rotaru AE. 2020. Extracellular electron uptake in *Methanosarcinales* is
557 independent of multiheme *c*-type cytochromes. Sci Rep 10.
558 20. Zheng S, Liu F, Wang B, Zhang Y, Lovley DR. 2020. Methanobacterium Capable
559 of Direct Interspecies Electron Transfer. Environ Sci Technol 54:15347-15354.
560 21. Holmes DE, Rotaru AE, Ueki T, Shrestha PM, Ferry JG, Lovley DR. 2018.
561 Electron and Proton Flux for Carbon Dioxide Reduction in Methanosarcina
562 barkeri During Direct Interspecies Electron Transfer. Front Microbiol 9:3109.

bioRxiv preprint doi: https://doi.org/10.1101/2021.06.11.448114; this version posted June 11, 2021. The copyright holder for this preprint (which was not certified by peer review) is the author/funder, who has granted bioRxiv a license to display the preprint in perpetuity. It is made available under aCC-BY-NC-ND 4.0 International license.

563 22. Zhou J, Holmes D, Tang H, Lovley D. 2021. Correlation of key physiological
564 properties of *Methanosarcina* isolates with environment of origin. Appl Environ
565 Microbiol doi:10.1128/AEM.00731-21:00731-21.
566 23. Yee MO, Snoeyenbos-West OL, Thamdrup B, Ottosen LDM, Rotaru AE. 2019.
567 Extracellular electron uptake by two *Methanosarcina* species. Front Energy Res
568 7.
569 24. Kletzin A, Heimerl T, Flechsler J, van Niftrik L, Rachel R, Klingl A. 2015.
570 Cytochromes *c* in Archaea: distribution, maturation, cell architecture, and the
571 special case of Ignicoccus hospitalis. Front Microbiol 6.
572 25. Ferry JG. 2020. Methanosarcina acetivorans: A Model for Mechanistic
573 Understanding of Aceticlastic and Reverse Methanogenesis. Front Microbiol
574 11:1806.
575 26. Buan N, Kulkarni G, Metcalf W. 2011. Genetic methods for *methanosarcina*
576 species. Meth Enzymol 494:23-42.
577 27. Metcalf WW, Zhang JK, Apolinario E, Sowers KR, Wolfe RS. 1997. A genetic
578 system for Archaea of the genus Methanosarcina: liposome-mediated
579 transformation and construction of shuttle vectors. Proc Natl Acad Sci U S A
580 94:2626-31.
581 28. Nayak DD, Metcalf WW. 2017. Cas9-mediated genome editing in the
582 methanogenic archaeon Methanosarcina acetivorans. Proc Natl Acad Sci U S A
583 114:2976-2981.
584 29. Holmes DE, Ueki T, Tang HY, Zhou J, Smith JA, Chaput G, Lovley DR. 2019. A
585 membrane-bound cytochrome enables *Methanosarcina acetivorans* to conserve
586 energy from extracellular electron transfer. mBio 10:e00789-19.
587 30. Summers ZM, Fogarty HE, Leang C, Franks AE, Malvankar NS, Lovley DR.
588 2010. Direct exchange of electrons within aggregates of an evolved syntrophic
589 coculture of anaerobic bacteria. Science 330:1413-5.
590 31. Rotaru AE, Shrestha PM, Liu FH, Shrestha M, Shrestha D, Embree M, Zengler K,
591 Wardman C, Nevin KP, Lovley DR. 2014. A new model for electron flow during
592 anaerobic digestion: direct interspecies electron transfer to Methanosaeta for the
593 reduction of carbon dioxide to methane. Energy Environ Sci 7:408-415.
594 32. Shrestha PM, Rotaru AE, Summers ZM, Shrestha M, Liu F, Lovley DR. 2013.
595 Transcriptomic and genetic analysis of direct interspecies electron transfer. Appl
596 Environ Microbiol 79:2397-404.
597 33. Sowers KR, Baron SF, Ferry JG. 1984. Methanosarcina acetivorans sp. nov., an
598 Acetotrophic Methane-Producing Bacterium Isolated from Marine Sediments.
599 Appl Environ Microbiol 47:971-8.
600 34. Chen S, Rotaru AE, Liu F, Philips J, Woodard TL, Nevin KP, Lovley DR. 2014.
601 Carbon cloth stimulates direct interspecies electron transfer in syntrophic co-
602 cultures. Bioresour Technol 173:82-6.
603 35. Chen S, Rotaru AE, Shrestha PM, Malvankar NS, Liu F, Fan W, Nevin KP,
604 Lovley DR. 2014. Promoting interspecies electron transfer with biochar. Sci Rep
605 4:5019.
606 36. Liu F, Rotaru A, Shrestha P, Malvankar N, Nevin K, Lovley D. 2012. Promoting
607 direct interspecies electron transfer with activated carbon. Energy Environ Sci
608 5:8982-8989.

bioRxiv preprint doi: https://doi.org/10.1101/2021.06.11.448114; this version posted June 11, 2021. The copyright holder for this preprint (which was not certified by peer review) is the author/funder, who has granted bioRxiv a license to display the preprint in perpetuity. It is made available under aCC-BY-NC-ND 4.0 International license.

609 37. Ueki T, Nevin K, Rotaru A, Wang L, Woodard T, Lovley DR. 2018. *Geobacter*
610 strains expressing poorly conductive pili reveal constraints on direct interspecies
611 electron transfer mechanisms. mBio 9:e01273-18.
612 38. Beeby M, Ferreira JL, Tripp P, Albers SV, Mitchell DR. 2020. Propulsive
613 nanomachines: the convergent evolution of archaella, flagella and cilia. FEMS
614 Microbiol Rev 44:253-304.
615 39. Walker D, Martz E, Holmes D, Zhou Z, Nonnenmann S, Lovley D. 2019. The
616 Archaellum of Methanospirillum hungatei Is Electrically Conductive. mBio
617 10:e00579-19.
618 40. Jarrell K, Albers S, de Sousa Machado J. 2021. A comprehensive history of
619 motility and archaellation in Archaea. FEMS Microbes 2.
620 41. Li Q, Li L, Rejtar T, Lessner DJ, Karger BL, Ferry JG. 2006. Electron transport in
621 the pathway of acetate conversion to methane in the marine archaeon
622 Methanosarcina acetivorans. J Bacteriol 188:702-10.
623 42. Schlegel K, Welte C, Deppenmeier U, Muller V. 2012. Electron transport during
624 aceticlastic methanogenesis by Methanosarcina acetivorans involves a sodium-
625 translocating Rnf complex. FEBS J 279:4444-52.
626 43. Suharti S, Wang M, de Vries S, Ferry JG. 2014. Characterization of the RnfB and
627 RnfG subunits of the Rnf complex from the archaeon Methanosarcina
628 acetivorans. PLoS One 9:e97966.
629 44. Wang M, Tomb JF, Ferry JG. 2011. Electron transport in acetate-grown
630 Methanosarcina acetivorans. BMC Microbiol 11:165.
631 45. Welte C, Deppenmeier U. 2014. Bioenergetics and anaerobic respiratory chains of
632 aceticlastic methanogens. Biochimica Et Biophysica Acta-Bioenergetics
633 1837:1130-1147.
634 46. Prakash D, Chauhan SS, Ferry JG. 2019. Life on the thermodynamic edge:
635 Respiratory growth of an acetotrophic methanogen. Sci Adv 5:eaaw9059.
636 47. Prakash D, Iyer PR, Suharti S, Walters KA, Santiago-Martinez MG, Golbeck JH,
637 Murakami KS, Ferry JG. 2019. Structure and function of an unusual flavodoxin
638 from the domain Archaea. Proc Natl Acad Sci U S A 116:25917-25922.
639 48. Beifuss U, Tietze M, Baumer S, Deppenmeier U. 2000. Methanophenazine:
640 strucrture, total synthesis, and function of a new cofactor from methanogenic
641 archaea. Angew Chem Int Ed 39:2470-2471.
642 49. Abken HJ, Tietze M, Brodersen J, Baumer S, Beifuss U, Deppenmeier U. 1998.
643 Isolation and characterization of methanophenazine and function of phenazines in
644 membrane-bound electron transport of *Methanosarcina mazei* Gol. J Bacteriol
645 180:2027-2032.
646 50. Ogawa T, Yoshimura T, Hemmi H. 2010. Geranylfarnesyl diphosphate synthase
647 from *Methanosarcina mazei*: different role, different evolution. Biochem Biophys
648 Res Commun 393:16-20.
649 51. Thauer RK, Kaster AK, Seedorf H, Buckel W, Hedderich R. 2008. Methanogenic
650 archaea: ecologically relevant differences in energy conservation. Nat Rev
651 Microbiol 6:579-91.
652 52. Mand T, Kulkarni G, Metcalf W. 2018. Genetic, biochemical, and molecular
653 characterization of Methanosarcina barkeri mutants lacking three distinct classes
654 of hydrogenase. J Bacteriol 200:e00342-18.

bioRxiv preprint doi: https://doi.org/10.1101/2021.06.11.448114; this version posted June 11, 2021. The copyright holder for this preprint (which was not certified by peer review) is the author/funder, who has granted bioRxiv a license to display the preprint in perpetuity. It is made available under aCC-BY-NC-ND 4.0 International license.

655 53. Yan Z, Ferry J. 2018. Electron bifurcation and confurcation in methanogenesis
656 and reverse methanogenesis. Front Microbiol 9:1322.
657 54. Yan Z, Wang MY, Ferry JG. 2017. A ferredoxin-and F420H2-dependent,
658 electron-bifurcating, heterodisulfide reductase with homologs in the domains
659 *bacteria* and *archaea*. mBio 8:e02285-16.
660 55. Jasso-Chavez R, Apolinario EE, Sowers KR, Ferry JG. 2013. MrpA functions in
661 energy conversion during acetate-dependent growth of Methanosarcina
662 acetivorans. J Bacteriol 195:3987-94.
663 56. Jasso-Chavez R, Diaz-Perez C, Rodriguez-Zavala JS, Ferry JG. 2017. Functional
664 role of MrpA in the MrpABCDEFG Na+/H+ antiporter complex from the
665 archaeon *Methanosarcina acetivorans*. J Bacteriol 199:e00662-16.
666 57. Lovley DR, Giovannoni SJ, White DC, Champine JE, Phillips EJ, Gorby YA,
667 Goodwin S. 1993. Geobacter metallireducens gen. nov. sp. nov., a microorganism
668 capable of coupling the complete oxidation of organic compounds to the
669 reduction of iron and other metals. Arch Microbiol 159:336-44.
670 58. Pritchett MA, Zhang JK, Metcalf WW. 2004. Development of a markerless
671 genetic exchange method for Methanosarcina acetivorans C2A and its use in
672 construction of new genetic tools for methanogenic archaea. Appl Environ
673 Microbiol 70:1425-33.
674 59. Sowers KR, Boone JE, Gunsalus RP. 1993. Disaggregation of *Methanosarcina*
675 spp. and growth as single cells at elevated osmolarity. Appl Environ Microbiol
676 59:3832-3839.
677 60. Holmes DE, Giloteaux L, Orellana R, Williams KH, Robbins MJ, Lovley DR.
678 2014. Methane production from protozoan endosymbionts following stimulation
679 of microbial metabolism within subsurface sediments. Front Microbiol 5.
680 61. Holmes DE, Risso C, Smith JA, Lovley DR. 2012. Genome-scale analysis of
681 anaerobic benzoate and phenol metabolism in the hyperthermophilic archaeon
682 Ferroglobus placidus. ISME J 6:146-57.
683 62. Bolger AM, Lohse M, Usadel B. 2014. Trimmomatic: a flexible trimmer for
684 Illumina sequence data. Bioinformatics 30:2114-20.
685 63. Magoc T, Salzberg SL. 2011. FLASH: fast length adjustment of short reads to
686 improve genome assemblies. Bioinformatics 27:2957-63.
687 64. Kopylova E, Noe L, Touzet H. 2012. SortMeRNA: fast and accurate filtering of
688 ribosomal RNAs in metatranscriptomic data. Bioinformatics 28:3211-7.
689 65. Robinson MD, McCarthy DJ, Smyth GK. 2010. edgeR: a Bioconductor package
690 for differential expression analysis of digital gene expression data. Bioinformatics
691 26:139-40.
692

693 **Figure Legends**

694 **Figure 1**. Ethanol consumption and production of methane and acetate in co-cultures

695 established with *G. metallireducens* and *M. acetivorans* after four

bioRxiv preprint doi: https://doi.org/10.1101/2021.06.11.448114; this version posted June 11, 2021. The copyright holder for this preprint (which was not certified by peer review) is the author/funder, who has granted bioRxiv a license to display the preprint in perpetuity. It is made available under aCC-BY-NC-ND 4.0 International license.

696 successive transfers. Data are means and standard deviation of triplicate
697 cultures.

698 **Figure 2**. Model for electron and proton flux in *Methanosarcina acetivorans* during
699 direct interspecies electron transfer (DIET) with *Geobacter*
700 *metallireducens*. Ethanol is provided as the source of electrons and the
701 electron-donating partner (*G. metallireducens*) transfers those electrons to
702 the electron-accepting partner (*M. acetivorans*) for carbon dioxide
703 reduction to CH_4 through the proposed pathways shown. The degree of
704 increased transcript abundance for subunits of the protein complexes is
705 provided. See main text for more detailed explanation.

706 **Figure 3**. Images of *G. metallireducens/M. acetivorans* co-cultures. (a) Confocal
707 microscopy image demonstrating aggregate size and cell distributions. (b-
708 f) Transmission electron micrographs. Arrows point to archaella extending
709 from the *M. acetivorans* surface. Abbreviations: M.a.: *M. acetivorans*;
710 G.m.: *G. metallireducens*.

711 **Figure 4.** Methane production during initial establishment of co-cultures with *G.*
712 *metallireducens* and various *M. acetivorans* strains grown with ethanol (20
713 mM) provided as the electron donor in the absence (a) or presence (b) of
714 granular activated carbon (GAC). Data are means and standard deviation
715 of triplicate cultures.
716 GM: wild-type *G. metallireducens*; MA: wild-type *M. acetivorans*;
717 Δ*mmcA*: *M. acetivorans* strain lacking the gene for the multi-heme

bioRxiv preprint doi: https://doi.org/10.1101/2021.06.11.448114; this version posted June 11, 2021. The copyright holder for this preprint (which was not certified by peer review) is the author/funder, who has granted bioRxiv a license to display the preprint in perpetuity. It is made available under aCC-BY-NC-ND 4.0 International license.

718 cytochrome MmcA; Δ*flaB1*Δ*flaB2*: *M. acetivorans* strain lacking the

719 genes for the archaellins FlaB1 and FlaB2.

720

bioRxiv preprint doi: https://doi.org/10.1101/2021.06.11.448114; this version posted June 11, 2021. The copyright holder for this preprint (which was not certified by peer review) is the author/funder, who has granted bioRxiv a license to display the preprint in perpetuity. It is made available under aCC-BY-NC-ND 4.0 International license.

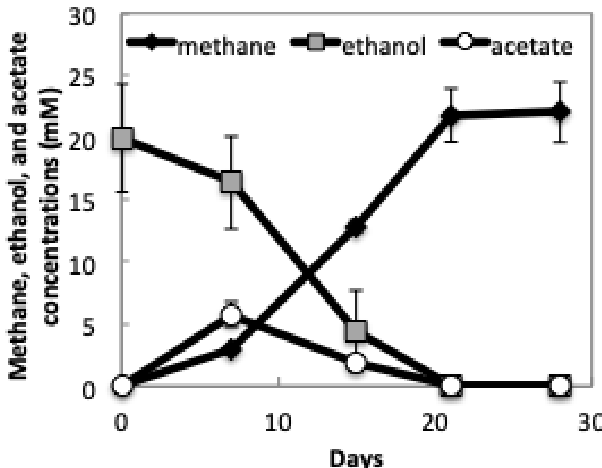

bioRxiv preprint doi: https://doi.org/10.1101/2021.06.11.448114; this version posted June 11, 2021. The copyright holder for this preprint (which was not certified by peer review) is the author/funder, who has granted bioRxiv a license to display the preprint in perpetuity. It is made available under aCC-BY-NC-ND 4.0 International license.

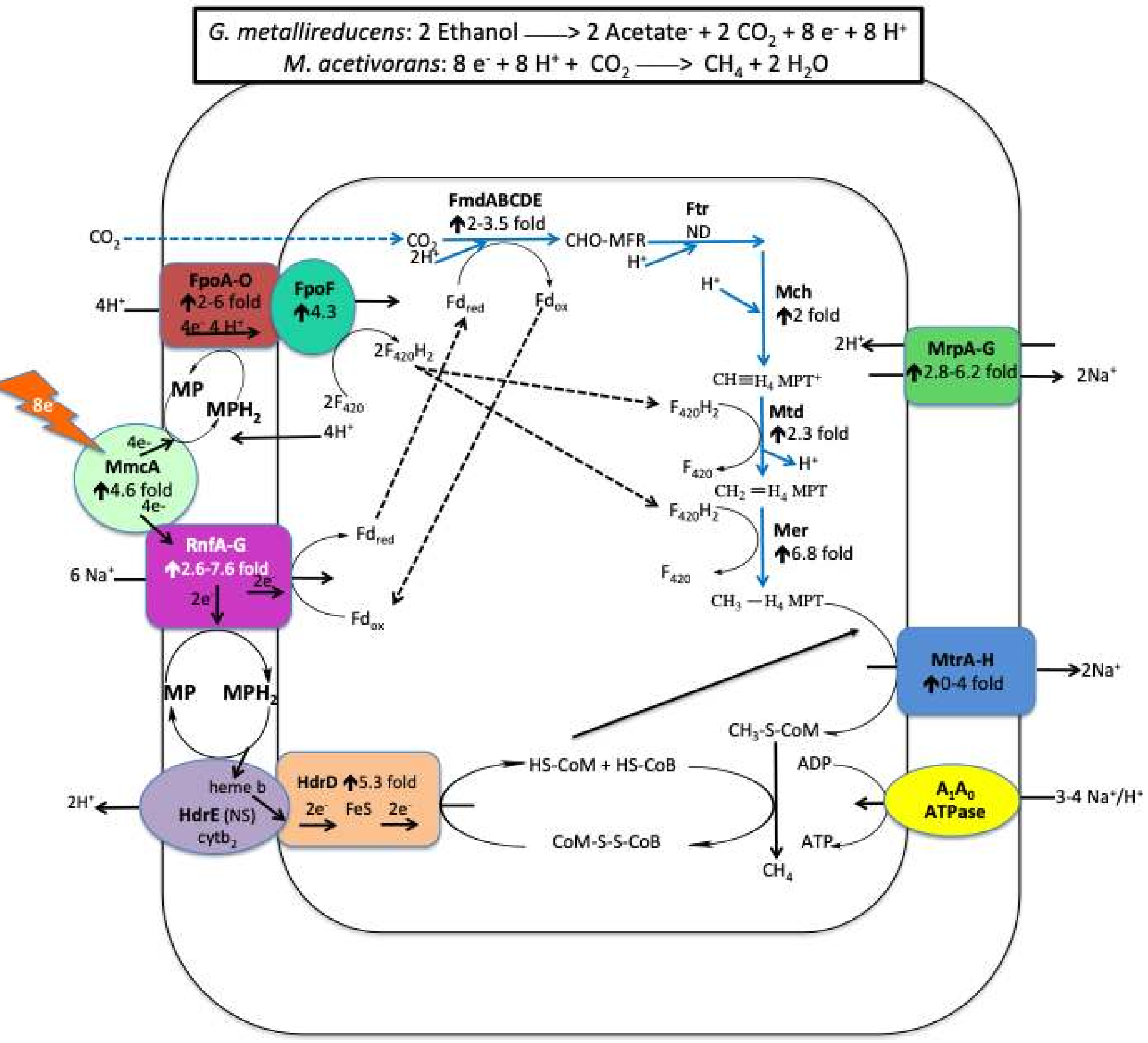

bioRxiv preprint doi: https://doi.org/10.1101/2021.06.11.448114; this version posted June 11, 2021. The copyright holder for this preprint (which was not certified by peer review) is the author/funder, who has granted bioRxiv a license to display the preprint in perpetuity. It is made available under aCC-BY-NC-ND 4.0 International license.

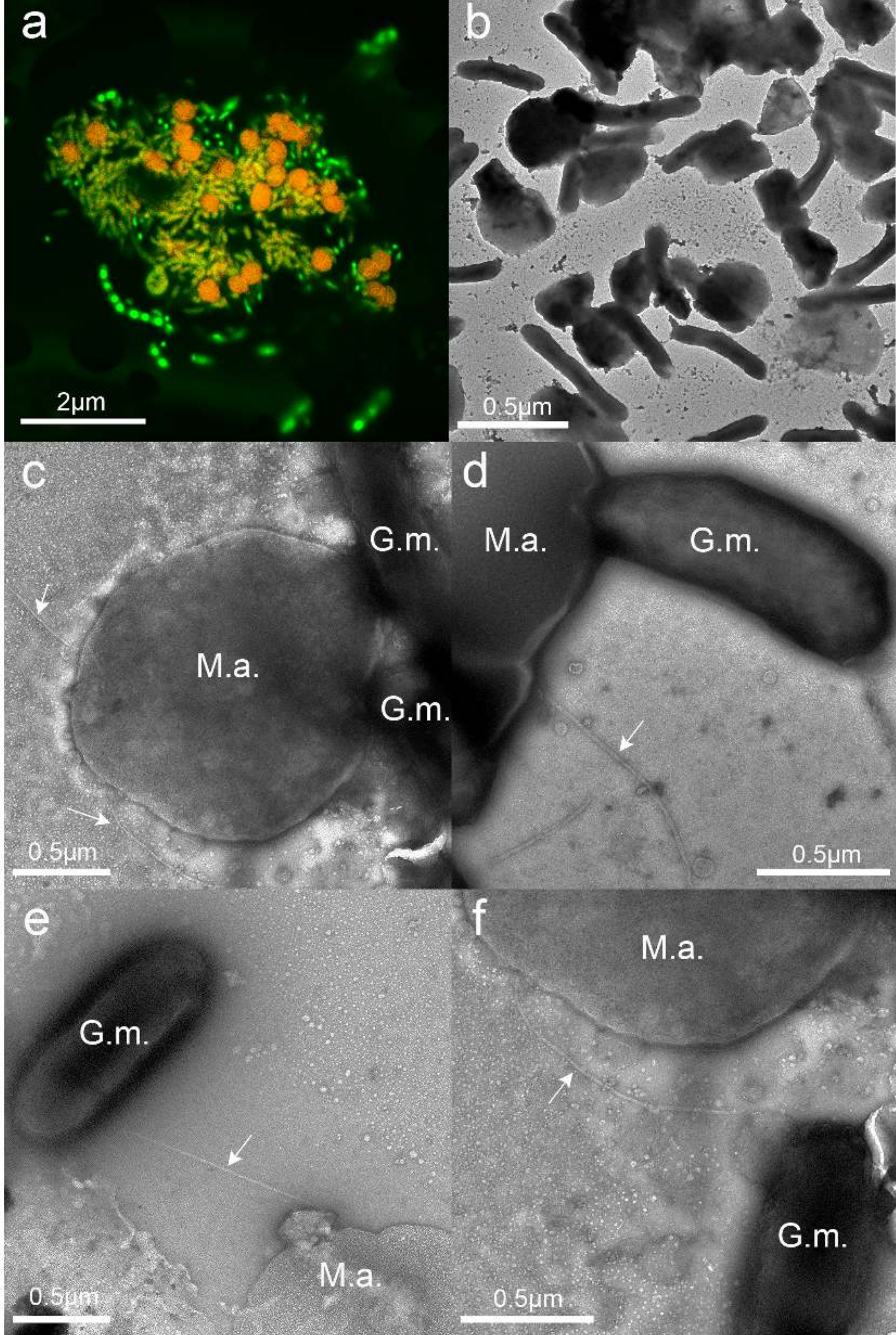

bioRxiv preprint doi: https://doi.org/10.1101/2021.06.11.448114; this version posted June 11, 2021. The copyright holder for this preprint (which was not certified by peer review) is the author/funder, who has granted bioRxiv a license to display the preprint in perpetuity. It is made available under aCC-BY-NC-ND 4.0 International license.